

# Observations of capillary barriers and preferential flow in layered snow during cold laboratory experiments

Francesco Avanzi<sup>1</sup>, Hiroyuki Hirashima<sup>2</sup>, Satoru Yamaguchi<sup>2</sup>,  
Takafumi Katsushima<sup>3</sup>, and Carlo De Michele<sup>1</sup>

<sup>1</sup>Department of Civil and Environmental Engineering, Politecnico di Milano, Milano, Italy

<sup>2</sup>Snow and Ice Research Center, National Research Institute for Earth Science and Disaster Resilience, Suyoshi-machi, Nagaoka-shi, Niigata-ken, 940-0821, Japan

<sup>3</sup>Meteorological Risk and Buffer Forest Laboratory, Department of Meteorological Environment, Forestry and Forest Products Research Institute, Tsukuba-shi, Ibaraki-ken, 305-8687, Japan

*Correspondence to:* Francesco Avanzi (francesco.avanzi@mail.polimi.it)

## Abstract.

We carried out observations of dyed water infiltration in layered snow during cold laboratory experiments. We considered three different finer-over-coarser textures and three different water input rates. Nine samples of layered snow were sieved and subjected to constant supply of tracer at 0°C. By means of visual inspection, horizontal sectioning, and measurements of liquid water content, capillary barriers and associated preferential flow were characterized. The dynamics of each sample were also simulated solving Richards equation within the 1D multi-layer physically-based SNOWPACK model. Results reveal that capillary barriers and preferential flow are relevant processes ruling the speed of liquid water in stratified snow. Both are marked by a high degree of spatial variability at cm scale and complex 3D patterns. During unsteady percolation of liquid water, observed peaks in bulk volumetric liquid water content (LWC) at the interface reach  $\sim 33 - 36$  vol% when the upper layer is composed by fine snow (grain size smaller than 0.5 mm). A comparison with expected wetness at water entry suction suggests that LWC might locally reach saturated conditions. Spatial variability in water transmission increases with grain size, whereas we did not observe a systematic dependency on water input rate for samples containing fine snow. The comparison between observed and simulated LWC profiles reveals that the implementation of Richards equation reproduces the existence of a capillary barrier for all observed cases and yields a good agreement with observed peaks in LWC at the interface between layers.

## 1 Introduction

Liquid water movement in snow rules streamflow timing and amount (Lundquist and Dettinger, 2005; Lehning et al., 2006; Wever et al., 2014), snowpack mechanical properties and stability in wet

conditions (Marshall et al., 1999; Baggi and Schweizer, 2008; Mitterer et al., 2011; Techel et al., 2011; Mitterer and Schweizer, 2013; Mitterer et al., 2013; Schmid et al., 2015), and snow albedo (Dietz et al., 2012). Furthermore, Harper et al. (2012); Forster et al. (2014); Machguth et al. (2016) report that meltwater percolation - storage dynamics in snow and firn might play an important role in determining the timing of sea - level rise by Climate Change. Liquid water in snow can be measured as a volumetric fraction (LWC, or  $\theta$ ), i.e., the ratio between liquid water volume and total snow volume (Fierz et al., 2009). LWC is usually expressed in vol %, or %.

Water flow in snow emerges as a complex, 3D process when observed in the field or in the laboratory. The co-existence of water and ice grains causes fast metamorphism (Brun, 1989) and phase change, which leads to melt-freeze and to the possible development of ice lenses when water infiltrates in subfreezing snow (Pfeffer and Humphrey, 1996). The interaction with topography can redistribute water at slope scale (Eiriksson et al., 2013). Moreover, water movement is usually marked by high spatial variability due to the occurrence of preferential flow, or fingering (Marsh and Woo, 1984a, 1985; McGurk and Marsh, 1995; Schneebeli, 1995; Waldner et al., 2004; Williams et al., 2010; Katsushima et al., 2013). These processes deeply complicate the modeling of liquid water in snow, which has been often simplified in the past by using a simple Darcian theory that neglects effects of capillary gradients on the flow (Colbeck, 1972; Wankiewicz, 1978). In particular, fingering is deemed to play a key role in ruling water arrival time at snow base, hence runoff (Wever et al., 2014, 2015).

The exact physics of preferential flow in snow is still not known (Katsushima et al., 2013) and modeling strategies are therefore still preliminary. For instance, Marsh and Woo (1985) propose an explicit definition of multiple-path routes, whereas Katsushima et al. (2009a) introduce a threshold  $\theta$  triggering preferential runoff. Wever et al. (2014) report that solving Richards equation accounting for suction gradients improves run-off estimations at different temporal resolutions, but it also accelerates meltwater front progress if compared with data from an upGPR and simulations by a bucket scheme (Wever et al., 2015). This result has been attributed to an unexpected simulation of some effects of preferential flow by the water scheme used.

The use of Richards equation for modeling wetting front instability in porous media is still a matter of debate (Egorov et al., 2003; Waldner et al., 2004; DiCarlo, 2013) due to the occurrence of peculiar pore-scale processes when water infiltrates as fingers (Egorov et al., 2003; DiCarlo, 2013; Katsushima et al., 2013; Baver et al., 2014). Observations reveal that, in soils, an unstable infiltration profile may be marked by an overshoot profile in terms of  $\theta$  (saturation overshoot) or  $\psi$  (capillary pressure overshoot, see DiCarlo (2004, 2007, 2013); Baver et al. (2014)). Examples of pressure overshoots have been observed in homogeneous snow samples during preferential infiltration by Katsushima et al. (2013). In addition, Hirashima et al. (2014) report promising attempts to reproduce similar dynamics using a model; they show that including spatial heterogeneity of snow properties and water entry suction ( $\psi_{WE}$ ) in a 3D resolution of Richards equation enables to re-

construct preferential flow effects. These results suggest that preferential flow in isothermal snow at  
60 0°C might be explained (and modeled) basing on the theory of gravity-driven instability of fingers  
in soils (Katsushima et al., 2009b, 2013).

According to Hirashima et al. (2014), water entry suction is thus a key variable ruling preferential  
flow development, as it impedes the movement of water between dry and wet snow during  
wetting until suction reaches  $\psi_{WE}$ . This process causes local accumulation of liquid water at mi-  
65 crostructural discontinuities (henceforth, simply ponding). A decrease in  $\psi$  during ponding is caused  
by the fact that  $\theta$  and  $\psi$  are related by a hysteretic relation called Water Retention Curve, WRC  
(Daanen and Nieber, 2009; Yamaguchi et al., 2010; Adachi et al., 2012; Yamaguchi et al., 2012).  
Then, water infiltrates in locations marked by local heterogeneity, thus triggering preferential flow.

In layered snow, water entry suction is also the driving parameter ruling capillary barrier develop-  
70 ment (Baker and Hillel, 1990). This is a finer-over-coarser transition in layering that causes a pause  
in the undisturbed advancement of the wetting front, ponding, horizontal diversion of liquid water  
and a delay in the expected travel time of water. Hill and Parlange (1972); Baker and Hillel (1990);  
Hillel and Baker (1988) discuss this process in soils, whereas Wakahama (1963); Jordan (1995);  
Waldner et al. (2004); Peitzsch et al. (2008); Mitterer et al. (2011) report some examples in snow.  
75 In soils, Hillel and Baker (1988); Baker and Hillel (1990) note that, after reaching  $\psi_{WE}$ , subsequent  
flow in the coarser layer will be marked by fingers if, in steady conditions, the hydraulic conductivity  
of the lower layer at  $\psi_{WE}$  is greater than the flux through the top layer  $q$  (due to mass conservation).  
Thus, ponding of water above a capillary barrier is prone to subsequent flow instability, namely, to  
the development of preferential channels.

80 Capillary barriers can play an important role for triggering wet snow avalanches (Mitterer et al.,  
2011; Wever et al., 2016). For example, Wever et al. (2016) report that predicted local accumulations  
of liquid water like those expected during ponding at capillary barriers can be used to separate  
avalanche and non-avalanche days. The position of peak LWC within the snow cover correlates  
with avalanche size. These processes also affect the timing of snowmelt runoff (Wever et al., 2014).  
85 Furthermore, a thorough investigation of the properties of capillary barriers may help to gain a better  
understanding of the physics of water instability in snow in general, as water flow around these  
textural discontinuities is driven by  $\psi_{WE}$ . However, their characterization in the literature is still very  
limited (Eiriksson et al., 2013). Indeed, existing ad hoc observations in the laboratory or in the field  
consider a restricted variety of grain size ( $g_S$ ) combinations (Jordan, 1995; Waldner et al., 2004). In  
90 field conditions, LWC profiles are usually measured using destructive, manual methods that strongly  
limit the temporal and spatial resolution of profiles. Thus, the evaluation of promising results from  
physically-based models (Hirashima et al., 2010; Mitterer et al., 2011; Wever et al., 2014, 2015) are  
often hampered by a lack of a proper high-resolution experimental database.

Here, we focus on observing capillary barriers and associated preferential flow in snow using  
95 laboratory experiments. We collected systematic observations of dyed water infiltration in layered

snow samples with different grain size combinations and different water input rates. We measured, for each sample, the thickness of the volume of the upper layer affected by ponding of water at the textural boundary, LWC profiles, wet snow fraction at different depths, and the arrival time of liquid water at sample base. These experiments were performed choosing a quite high vertical  
100 resolution of all the measurements (2 cm) and a broad set of input rates and textures, thus enabling a quantitative characterization of capillary barriers properties that is more exhaustive than before. All the laboratory experiments are compared with numerical simulations of Richards equation in snow by the 1D multi-layer physically-based SNOWPACK model.

We consider isothermal conditions at  $0^{\circ}\text{C}$ , thus avoiding any investigation about wetting front advancement in subfreezing snow, which presents additional challenges. As an example, Marsh and Woo  
105 (1984a, b) report that zones with mixed wet and dry snow develop in such conditions (see also Pfeffer et al. (1990); Pfeffer and Humphrey (1996)). The impact of these processes on runoff response time of snow in sub-freezing conditions is still a matter of debate (Marsh and Woo, 1984b), especially on seasonal time scales (Wever et al., 2014).

## 110 2 Methods

### 2.1 Preparation of samples

The main prerequisite to observe capillary barriers in initially dry snow is a finer-over-coarser profile in layering. For this purpose, three combinations of grain size were considered here: 1) FC, i.e., fine-over-coarse snow; 2) FM, i.e., fine-over-medium snow; 3) MC, i.e., medium-over-coarse  
115 snow. We classify snow with  $0.25\text{ mm} \leq g_S \leq 0.5\text{ mm}$  as fine, snow with  $1\text{ mm} \leq g_S \leq 1.4\text{ mm}$  as medium, and snow with  $2\text{ mm} \leq g_S \leq 2.8\text{ mm}$  as coarse. Note that this nomenclature is convenient for the scopes of this paper, but it is not consistent with the International Classification proposed by Fierz et al. (2009), which for instance defines medium snow grain size as  $0.5\text{ mm} \leq g_S \leq 1\text{ mm}$ .

Experimental evidences reveal that the area occupied by fingers in snow (Katsushima et al., 2013)  
120 and the value of  $\psi_{WE}$  (DiCarlo, 2007; Katsushima et al., 2013) may be both functions of water input rate. In order for our conclusions to be more general, we carried out experiments with three different water inputs  $W$ : these are  $\sim 10, 30$  and  $100\text{ mm/h}$ . These water input rates are a compromise between the need for exploring the properties of capillary barriers over a broad range of  $W$ , expected melt rates in natural conditions (DeWalle and Rango, 2011), and operational constraints  
125 (specifically, expected duration of the tests). Note that Katsushima et al. (2013) has already observed preferential infiltration in snow with average  $g_S$  between  $0.421 - 1.439\text{ mm}$  for different water input rates ( $21.7\text{ mm/h} \leq W \leq 205.5\text{ mm/h}$ ). Thus, we did not consider any instability criterion (Saffman and Taylor, 1958; Baker and Hillel, 1990; de Rooij, 2000; DiCarlo, 2013) while designing our experiments.

130 Nine samples were prepared in a cold room at  $-20^{\circ}\text{C}$  using refrozen melt forms (one sample for each of the three grain size combinations and three water input rates). Henceforth, numbers 1, 2 and 3 differentiate samples with same grain size combination, but subjected to different water input rate (10, 30 and 100 mm/h, respectively). Fragmented snow particles were firstly partitioned in several classes of grain size. Afterwards, the three  $g_S$  chosen were sieved a second time to prepare the  
135 samples. Snow was packed in a cylindrical container. The container was composed by a number of acrylic rings (height equal to 20 mm, diameter equal to 50 mm) that were previously taped on the external side. After sieving the lower layer, its dry density ( $\rho_{D,L}$ ) was measured by gravimetry. The dry density of the upper layer ( $\rho_{D,U}$ ) was measured by gravimetry at the end of sieving operations (by considering the difference between sample total weight and sample weight before sieving the  
140 upper layer). After preparation, each sample was moved to a second cold room at  $0^{\circ}\text{C}$ , where it was stored for at least 12 hours to reach initial conditions of dry snow at  $0^{\circ}\text{C}$ .

We report in Table 1 the details of each experiment. Water input rates are reported both in mm/h and in g/min (samples diameter equal to 5 cm). The coefficients of variation of  $\rho_{D,U}$  and  $\rho_{D,L}$  read 0.06 and 0.03. We did not apply any tamping during sieving operations so we had no direct control  
145 on the values of  $\rho_{D,U}$  and  $\rho_{D,L}$ . Given the low variability of these two variables, we point out that this work investigates how capillary barrier effects and associated preferential flow vary with grain size only. Future investigations should focus on the generalization of this work to layers of different density. Some samples (namely, FC2, FM2 and MC2) are shorter than the others. However, the thickness of the upper layer is the same for all the samples. This is important as ponding occurs in  
150 the upper layer.

## 2.2 Data collection

Before starting each experiment, we placed a thin cotton ring on the top of the sample to enable the point source of the tracer to spread over the surface of the upper layer. Then, each experiment was started by supplying dyed water into samples using a micro-tube pump. The dye used was blue  
155 ink, diluted by a factor of 10 times in water at  $0^{\circ}\text{C}$ . We monitored  $W$  during each experiment by automatically measuring the weight of the tracer reservoir (1 minute resolution). Absolute relative differences between experimental (Table 1) and reference (10, 30 and 100 mm/h) values of  $W$  range between 6% - 19% as it is difficult to apply a constant, low input rate.

When the tracer reached the base of each sample, tracer supply was stopped. The arrival time of  
160 the tracer at sample base ( $t_t$ ) was registered with a manual chronometer watch by visually inspecting samples during the experiments. Since samples had different heights, we define a specific travel time,

$$\tau = t_t/h, \tag{1}$$

with  $h$  equal to sample height. Note that  $\tau$  is in min/cm as it is the reciprocal of velocity. After each experiment, pictures of the external sides of the sample were taken to estimate the approximate thickness of the upper layer marked by liquid water accumulation ( $p$ , in cm). Soon afterwards, we took pictures of the top section of each acrylic ring (by gradually removing them from the column, snow included). At the same time, the liquid water mass  $w$ , in grams, in each of the rings was measured using a portable calorimeter (Kawashima et al., 1998). These measurements were translated into profiles of volumetric liquid water content by converting  $w$  to  $\theta$ . Fractions of wet areas over total area ( $f$ ) were also estimated for each section by manually delimiting fingers in all the pictures taken and calculating their extension using the ImageJ software (<http://imagej.nih.gov/ij/>, 1.48 v, see Abramoff et al. (2004)). Clearly, similar calculations may be performed using alternative software.

### 2.3 The comparison with SNOWPACK

We simulated the dynamics of each sample using the 1D multi-layer model SNOWPACK (Bartelt and Lehning, 2002). These simulations aim at comparing observations of capillary barrier development with predictions by a physically-based model, as previously done by, e.g., Hirashima et al. (2010); Mitterer et al. (2011); Wever et al. (2015) mainly using field observations. The relatively high-resolution of LWC measurements (2 cm) enables a detailed discussion of both, the physical process and its simulation by a operation model. This comparison will not include preferential flow patterns, as the model is 1D.

The model discretizes snow using a finite element grid. It simulates the evolution in time of a broad set of variables along a vertical profile of snow starting from external forcings. The original version of SNOWPACK considers a bucket-type approach to simulate liquid water percolation in snow. Accordingly, liquid water is retained at a given position in the profile until it exceeds a threshold (see Bartelt and Lehning (2002)). After exceeding, excess water is transmitted downwards. Hirashima et al. (2010) have introduced in SNOWPACK a water transport model based on the model by van Genuchten (1980) and on an equilibrium approximation of water flow to tackle numerical instability (see Hirashima et al. (2010) for details). Recently, Wever et al. (2014) have also introduced a discretization of Richards equation that significantly improves several aspects of liquid water simulation in snow. We used the numerical scheme by Wever et al. (2014) in this paper (WE, SNOWPACK version 3.3).

The initial spatial resolution of simulations was set to 2 cm. The time step was set to 1 minute, but the numerical scheme by Wever et al. (2014) reduces this initial time step basing on an iteration rule (see Wever et al. (2014) for details). Snow initial conditions were chosen to replicate the granulometry, density (Table 1),  $\theta$  (initially dry), and temperature ( $0^{\circ}\text{C}$ ) of the physical samples. Using the same sieves that we used here, Katsushima et al. (2013) obtained a mean grain size (hereinafter,  $\bar{g}_S$ ) for the class 0.25 - 0.5 mm and the class 1 - 1.4 mm equal to 0.406 mm and 1.463 mm, respectively.  $\bar{g}_S$  for medium snow is greater than the upper boundary of the sieve probably because snow grains

used were not perfectly spherical. In the simulation, we therefore set  $\bar{g}_S = 0.406$  mm for fine snow, 200  $\bar{g}_S = 1.463$  mm for medium snow and  $\bar{g}_S = 2.926$  mm for coarse snow (by assuming this last value as two times the average medium grain size). Bond size was assumed equal to one third of grain radius. Input data were chosen to replicate experimental conditions in the cold chamber, i.e., a constant precipitation flux (equal to the measured water input flux  $W$ , see Table 1) and a fixed air temperature of  $+0^\circ\text{C}$ . The threshold temperature for classifying solid and liquid events was set to  $-0.01^\circ\text{C}$ , in order 205 for  $W$  to be classified as liquid. Wind speed and solar radiation were set to zero, while incoming longwave radiation was calculated as  $\sigma T^4$ , where  $\sigma = 5.67 \cdot 10^{-8} \text{ W m}^{-2} \text{ K}^{-4}$ , and  $T = 273.15\text{K}$ . Parametrizations for snow permeability, unsaturated hydraulic conductivity, water retention curve, residual water content and averaging method for hydraulic conductivity at the interface were all kept at the default settings discussed for SNOWPACK in Wever et al. (2014, 2015).

210 Particular attention is paid to the comparison between observed and simulated LWC peak over the interface between layers, as this is an important variable involved in capillary barrier formation and in wet snow avalanche forecasting (Wever et al., 2016). Another key feature of capillary barriers is the vertical profile in LWC, which usually shows sharp variations with depth (Hirashima et al., 2010). However, choosing a precise snapshot of simulated LWC for the comparison with our observations 215 is difficult, as the model is 1D and, at this stage, does not include an explicit treatment of preferential flow patterns. These are expected to play a key role in water flow around capillary barriers as water concentrates in fingers that are characterized by a higher-than-average unsaturated hydraulic conductivity (due to a higher-than-average LWC). It follows that restricting this comparison to a single profile may be misleading as possible differences between observations and simulations might be 220 due to a process that is currently not treated by the model; this would severely limit the comparison. Thus, we will compare observed profiles of LWC with both, i) the simulated profile at the observed arrival time of water at sample base (WE1), and ii) the simulated profile at the arrival time of water in the model (WE2), which is chosen by identifying the instant when  $\theta$  at sample base reaches  $\sim 3$  vol% in the simulation (Mitterer et al., 2011).

225 On the one hand, WE1 is advantageous as supplied mass in experiments and in simulations matches, because both profiles refer to the same time step. On the other hand, flow in the lower layer will be at the beginning spatially variable, strongly accelerated and highly fingered (Katsushima et al., 2013), which are all features that are not explicitly included in a 1D model and that might hamper the application of Richards equation. Thus, when considering WE1, we will focus on the profile over the 230 interface, where the peak of LWC develops. Conversely, WE2 enables a comparison of a full profile of LWC, but the simulated mass of liquid water will be greater than observed due to the possible mismatch between observed and expected arrival time of water in simulations (Wever et al., 2014). This is particularly evident in the upper layer of FC and FM samples, as water speed in fine snow during matrix flow is slow. Thus, when considering WE2, we will focus on the profile in the lower

235 layer. We suggest that additional investigations should be carried out to establish proper frameworks  
for the high-resolution comparison of complex models and laboratory (or field) observations.

### 3 Results and Discussion

#### 3.1 Overview

Figure 1 reports the horizontal sections of all the samples (2 cm vertical resolution) at the end of  
240 the experiments (i.e., when dyed water arrived at sample base). Dyed water is visible as blue stains.  
Generally, the darker the color is, the higher is local LWC (Waldner et al., 2004). We report in Figure  
2 three examples of samples at the end of the experiment. These are FC2 (as an example of FC tests),  
FM2 (as an example of FM experiments) and MC1 (as an example of MC experiments).

Table 2 reports observations in terms of thickness of the upper layer marked by liquid water  
245 accumulation ( $p$ ), arrival time of water at the base of each sample ( $t_t$ ), and specific travel time of  
liquid water in snow ( $\tau$ ). In Figures 3 and 4, profiles of wet snow fractions  $f$  and LWC are given. In  
Fig. 4, each point represents bulk LWC in the underlying 2 cm. As an example, any value reported  
at a depth equal to 8 cm is bulk LWC between 8 cm and 10 cm. This represents the LWC measured  
immediately over the interface between layers.

250 Figure 5 compares observed and SNOWPACK-based profiles of volumetric LWC for each sample.  
Each point represents bulk LWC in the underlying 2 cm. As described in Section 2, two simulated  
profiles are reported (WE1 and WE2). When considering MC samples, we note that the total duration  
of experiments is very short (see Table 2) compared with FC and FM samples. Thus, we plotted only  
WE2 as the expected mismatch between supplied and simulated liquid water mass is limited.

#### 255 3.2 Development of capillary barriers

Fig. 1 confirms that liquid water movement through a finer-over-coarser snow texture is subjected  
to ponding and horizontal diversion of water when the wetting front comes to the textural interface.  
In FC and FM samples, horizontal spreading of water at the interface introduces a clear textural  
transition in wetness between finer and coarser layers (see Fig. 2). In 4 out of 6 samples of these two  
260 classes, a homogeneously blue area is observed even at a depth equal to 8 cm (i.e., 2 cm above the  
interface). MC samples show a more variable behavior. In fact, water spreading is spatially restricted  
for MC1 (see also Fig. 2), whereas marked horizontal redistribution of water is visible in MC2 and  
MC3. MC samples show a smaller  $p$  than FC and FM samples.

The difference between FC-FM and MC samples in terms of ponding behavior can be explained  
265 considering the retention properties of snow with different grain size.  $\psi_{WE}$  for medium and coarse  
snow can be estimated from grain size using the relation reported in Katsushima et al. (2013) and  
Hirashima et al. (2014):  $\psi_{WE} \sim 0.025$  m in coarse snow and  $\sim 0.04$  m in medium snow. Conversely,  
 $\psi$  in fine snow is  $\sim 0.22$  m ( $\theta = 5$  vol%) and  $0.21$  m ( $\theta = 10$  vol%), whereas  $\psi$  in medium snow



is  $\sim 0.09$  m ( $\theta = 5$  vol%) and  $0.08$  m ( $\theta = 10$  vol%). These approximate values of suction in snow  
270 were estimated using the WRC parametrization in snow by Yamaguchi et al. (2012), assuming an  
irreducible LWC equal to 2.4 vol % (Yamaguchi et al., 2010; Hirashima et al., 2014), and consider-  
ing 5 vol% and 10 vol% as reference values for relatively low saturation. Thus, in FC-FM samples  
the difference between  $\psi$  at relatively low saturation and  $\psi_{WE}$  is much greater than in MC sam-  
ples. Generally, the higher the difference between  $\psi$  in the upper layer and  $\psi_{WE}$  is, the larger is  
275 the mass of water accumulated and horizontally diverted. Note that the WRC by Yamaguchi et al.  
(2012) refers to a drying process and this may trigger some additional uncertainty when estimating  
 $\psi$  for a wetting process (see Section 3.4).

FC and FM samples are characterized by similar LWC profiles (Fig. 4). LWC increases with depth  
in the upper layer, it presents a marked peak at the textural boundary, and it decreases again below the  
280 capillary barrier. Peaks in LWC at the interface are a characteristic feature of capillary barriers as wa-  
ter ponds until  $\psi \rightarrow \psi_{WE}$ : similar examples are reported or discussed in, e.g., Waldner et al. (2004);  
Hirashima et al. (2010); Mitterer et al. (2011); Avanzi et al. (2015); Wever et al. (2015, 2016). All  
FC-FM samples yield a similar LWC in the upper layer at the interface:  $\sim 33$  vol% in FC samples  
and  $\sim 34$  vol% -  $36$  vol% in FM samples. This value is coupled with suction through a wetting curve  
285 (DiCarlo, 2007). This may be the reason why LWCs at the interface are similar, as  $\psi_{WE}$  is the same  
in all these six samples. Note that such values of LWC are much greater than those usually reported  
in field profiles (Fierz et al., 2009). LWC drives, among others, snow settling (Marshall et al., 1999)  
and wet snow metamorphism (Brun, 1989). Both processes experience a dramatic acceleration with  
increasing LWC. This supports the idea that capillary barriers may play an essential role for snow  
290 stability in wet conditions (Wever et al., 2016).

In MC samples, a smaller, but distinct, peak in LWC was measured at the interface: in MC1, LWC  
over the boundary is  $\sim 4.5$  vol%, whereas LWC values immediately above and below are 2.7 vol%  
and 1.7 vol%, respectively. In MC2 and MC3, the peak in LWC over the interface is  $\sim 9$  vol%. A  
smaller peak of LWC in MC layering is attributed to the small difference between  $\psi$  in medium snow  
295 and  $\psi_{WE}$  in coarse snow.

The occurrence of capillary barrier causes horizontal redistribution of water. Thus, spatial ho-  
mogenization of liquid water patterns at the interface is promoted. Indeed,  $f$  increases with depth  
over the boundary (where  $f = 1$  for all FC and FM samples, see Fig. 3). However, sections in Fig.  
1 reveal a remarkable spatial variability of this process at cm scale. For example, some pockets of  
300 dry snow persist at depths equal to 8 cm in samples FC2 and FC3 (i.e., 2 cm above the interface).  
Other hints are the observed spatial variability of  $p$  in each sample (Table 2) and the differences  
of coloring in some sections at depths equal to 8 or 10 cm (e.g., FC2, FC3 and FM3), as this is a  
signature of LWC (Waldner et al., 2004). Isolated clusters of liquid water surrounded by dry snow  
are also visible in MC1 and MC2. All these observations show that the distribution of liquid water  
305 above a capillary barrier has a marked 2/3D structure at local scale, probably due to heterogeneity in

snow microstructure. The difference in wet areas in MC samples for different water input rates might be on the contrary an effect of water input rate on  $\psi_{WE}$ , as observed in snow by Katsushima et al. (2013).

### 3.3 Preferential flow patterns and travel time of water in snow

310 Observed profiles of  $f$  suggest that liquid water movement in samples was marked by high spatial variability and that this variability is lower in fine snow layers than in medium or coarse snow. Overall, preferential flow turns out as the predominant pattern of liquid water infiltration in snow (Schneebeli, 1995). We observed that new fingers created during the percolation, and that sometimes fingers stopped their vertical percolation at some locations but continued to develop at others. The  
315 movement of fingers in the lower layer was very rapid and represented a small fraction of the total duration of each experiment (say, up to a few minutes even for slower input rates).

Katsushima et al. (2013) report that the total area of preferential flow (hence  $f$ ) in snow samples made by vertically homogeneous snow decreases with increasing grain size, but increases with increasing input flux. We also observed a decrease in  $f$  with increasing  $g_S$ , whereas a clear increase of  
320  $f$  with increasing  $W$  was detected only for MC samples. On the one hand, the expected dependency of  $f$  on sublayer unsaturated conductivity at  $\psi_{WE}$  (Hillel and Baker, 1988; Baker and Hillel, 1990) and the relation between  $\psi_{WE}$  and velocity (Weitz et al., 1987; DiCarlo, 2007; Katsushima et al., 2013) support the existence of a relation between  $f$  and  $W$  (albeit both effects have been mainly observed only in soils). On the other hand, these experiments included a capillary barrier, contrary  
325 to experiments by Katsushima et al. (2013), and this represents a major driver of liquid water patterns at local scale (see the previous Section). Accordingly, liquid water speed in the upper layer was locally affected by ponding, whereas inflow rate in the sublayer was driven by breakthrough of water at  $\psi_{WE}$ . Both processes limit the impact of external water input rate on  $f$ , at least until steady conditions are reached. In MC samples, the difference in retention properties between layers is lower;  
330 thus, the effect of a capillary barrier is spatially very localized. This may explain why observations in MC samples agree with previous observations in homogeneous snow.

Considering outcomes of different experiments in sand, DiCarlo (2013) reports that finger width might increase with both, very high (i.e., close to saturated conductivity) and very low supplied fluxes, while finger width keeps constant for a broad range of supplied flux in between. Water input  
335 rates in our experiments span 11 and 113 mm/h; these values are very small if compared with expected values of saturated conductivity in snow ( $\sim 10^4 - 10^6$  mm/h, see Katsushima et al. (2013)). We therefore suggest that future developments of this work should investigate the relation between flux and  $f$  extensively, i.e., enlarging the range of  $W$  considered during the experiments and/or reaching steady conditions.

340  $\tau$  increases with decreasing  $W$ , as clearly expected (Table 2). In the case of FM2 (fine over medium snow,  $W = 27.7$  mm/h), we can compare the  $\tau$  measured during the experiment (2.2

min/cm) with the  $\tau$  observed during the experiment by Katsushima et al. (2013), since this is the only  $g_S - W$  combination that these two works share. The  $\tau$  measured by Katsushima et al. (2013) for fine snow and  $W = 22.3$  mm/h is equal to 1.7 min/cm, while the  $\tau$  for medium snow and  $W = 21.7$  mm/h is equal to 0.7 min/cm. These results suggest that  $\tau$  in a FM sample is higher than the  $\tau$  observed in a homogeneous sample composed by medium snow. This is clearly expected since permeability in medium snow is higher than in fine snow. However, this  $\tau$  is even higher than the specific travel time observed in a homogeneous sample made by fine snow, which is less expected. This comparison helps to quantify the relevance of capillary effects in ruling water speed in snow and the arrival time of meltwater at snow base.

### 3.4 The comparison with SNOWPACK

Figure 5 shows promising results for the simulation of a capillary barrier. Indeed, the model clearly reproduces an increasing LWC with depth in the upper layer and a peak of LWC at the interface. Furthermore, LWC profiles below the barrier are generally in good agreement, once water has reached the base in the simulation. Point differences between observed and simulated LWC at the interface at WE1 read  $\sim 2 - 5$  vol% in FC1-FC2,  $\sim 3 - 8$  vol% in FM1-FM2, and  $\sim 0.1 - 5$  vol% in MC samples. As already mentioned, a good simulation of peak LWC is very important to correctly predict the occurrence of wet snow avalanches (Wever et al., 2016). A larger difference ( $\sim 9 - 13$  vol%) is found for higher input rates. However, note that FC3 and FM3 were subjected to an extremely high water input rate compared with natural conditions.

Previous evaluations of SNOWPACK already show that the inclusion of Darcy-Buckingham equation in snow enables a correct prediction of the onset of capillary barriers at textural discontinuities (Hirashima et al., 2010; Mitterer et al., 2011; Wever et al., 2015). Here, we enlarged previous findings by considering a broad set of snow textures and input rates, and a relatively high resolution of measurements.

Overall, observations show that both, breakthrough of liquid water below a capillary barrier and wet conditions in the upper layer or in fingers (Waldner et al., 2004) may present a proper process scale (Blöschl, 1999) of a few cm. This is because natural snow is spatially heterogeneous (Hirashima et al., 2014) and this may affect 3D patterns of capillary barriers (e.g., see the already discussed pockets of dry snow in FM3). Alternation of dry and wet snow can sensibly decrease the bulk LWC in a ring, although local LWC can still be very high. This may partially explain some differences between observations and 1D simulations. For example, predicted peak LWC in FC3 and FM3 is  $\sim 43 - 46$  vol%, which is close to saturated conditions (the porosity of fine snow in both samples is  $\sim 0.5$ ), but greater than observations. An approximate estimation of LWC at  $\psi_{WE}$  in fine snow (obtained assuming continuity of suction at the interface) reads 50 vol%, which is closer to SNOWPACK simulations than data. Thus, saturated conditions might be reached at local scale,

while bulk LWC (which is the effect of both, capillary barrier effects and snow heterogeneity in wetness at ring scale) can be lower.

Another example is water flow below the interface, which showed a high degree of spatial variability. The good agreement between the model and the data (at WE2) might suggest that, at this measurement scale, differences in LWC between a highly channeled flow and a matrix-only simulation balance, that is, fingers are usually highly saturated (Waldner et al., 2004), but occupy only a small fraction of total volume. Thus, the average LWC at ring scale is much lower than saturation and close to matrix conditions.

This result suggests that an exhaustive process understanding of the physics of capillary barriers in snow and water flow instability may need that a proper measurement and/or modeling scale are defined to clearly separate model-data significant discrepancies and effects due to the sampling strategy (see again Blöschl (1999) for a definition). Importantly, the measurement scale needed to capture 3D patterns of capillary barriers might be smaller than that usually used to sample LWC in the field (see again Fig. 1). Increasing the spatial resolution of LWC measurements is challenging as measuring LWC in snow is still marked by high uncertainties (Colbeck, 1978; Fierz and Föhn, 1995; Techel and Pielmeier, 2011; Avanzi et al., 2014). It is only recently that undisturbed, non-destructive and repetitive measurements of LWC have been obtained (Heilig et al., 2010; Schmid et al., 2015; Heilig et al., 2015; Kinar and Pomeroy, 2015). A promising alternative might be given by pore-scale measurements of liquid water flow (Adachi et al., 2012; Walter et al., 2013). This discussion also reveals the role played by heterogeneity (Hirashima et al., 2014) in introducing possible differences in LWC between 3D (bulk) and point (1D) conditions. Additional uncertainty may be caused by instrumental precision (see next Section), ambiguity in the identification of the correct snapshot of LWC for this comparison, and possible air trapped in voids at saturation (Yamaguchi et al., 2010).

Another important limitation for this discussion may be the present lack of an exhaustive investigation of WRC hysteresis in snow. Indeed, differences of LWC for a given suction are expected if hysteresis is explicitly taken into account. Furthermore, the absence of a proper parametrization of hysteresis may hamper the estimation of expected LWC at  $\psi_{WE}$  during ponding (i.e., wetting), if different WRCs for a wetting and a drying process are not known. Also, the hysteretic behavior of the WRC is considered an important factor in driving preferential flow in general, since for example it promotes the persistence of fingers in soils (Liu et al., 1994; DiCarlo, 2013). The magnitude of hysteresis is also related with the magnitude of capillary overshoot (Katsushima et al., 2013), although it is not the prime cause of instability (DiCarlo, 2013). At present, existing observations of hysteresis in snow are still very sparse (Adachi et al., 2012) and this represents an important limitation for interpreting existing results, although the WRC hysteresis of snow is expected to be smaller than the hysteresis of, e.g., sand (Katsushima et al., 2013).

### 3.5 The role of instrumental precision

A mass balance between supplied and measured liquid water mass reveals that the measured mass ranges between 93% and 176% of supplied mass in 8 out of 9 samples, while in MC1 measured  
415 mass is 434% of supplied mass. Note that in this last sample the total mass supplied is nonetheless very low due to the short duration of this experiment ( $\sim 2.88$  g).

This discrepancy can be explained by instrumental noise. Melting calorimetry has been widely used to measure LWC for decades (Yosida, 1960), but Colbeck (1978) points out that this method may be inaccurate as it implies the calculation of a difference between large numbers (Stein et al.,  
420 1997). According to Kinar and Pomeroy (2015), absolute errors in measuring LWC using calorimetry span 1% and 5%. The instrument we used here (the so-called Endo-type snow-water content meter) was proposed by Kawashima et al. (1998). They note that measured LWC span  $\pm 2\%$  of known LWC (by weight) in 87% of the cases. By comparing measurements by the Endo-type calorimeter with those by a dielectric device in snow pits (see Kawashima et al. (1998) for details), they note  
425 that this device returns alternatively higher or lower LWC if compared with high and low readings by the dielectric device.

We estimated an absolute error for these experiments by comparing the height-integrated LWC measured using calorimetry within each sample with the ratio between supplied liquid water volume and total volume of samples. The absolute difference spans 0.8 vol% and 2.97 vol%, thus it is consis-  
430 tent with the literature (Kinar and Pomeroy, 2015). Measured and simulated LWC by SNOWPACK are also in fairly agreement (see previous Section) and this is another good point since SNOWPACK bases on mass an energy conservation.

Capillary barriers and associated preferential flow represents a big challenge for LWC measure-  
435 ments. On the one hand, peaks in LWC at the interface are rather high and this is a problem for those instruments that may lose accuracy for high LWC, such as a Snow Fork (Techel and Pielmeier, 2011). On the other hand, bulk LWC in fingered snow may be very low, as water accelerates and occupies a small fraction of total volume. This means that such experiments need an instrument that guarantees a comparable performance for both, high and low LWC. This may represent a benefit of the Endo calorimeter (see Fig. 4 in Kawashima et al. (1998)), which seems also appropriate  
440 given the small dimension of each ring. Furthermore, Fierz and Föhn (1995) report that the absolute error in measuring water content using dielectric methods spans 0.2 and 0.9 vol%, while Techel and Pielmeier (2011) note that the expected difference between measurements taken using a Denoth meter and a Snow Fork is  $\sim 1$  vol%. Thus, measuring low LWCs is generally very challenging for several existing techniques. Finally, a highly fingered flow may be missed and/or  
445 disturbed by using bigger instruments, like TDRs (Stein et al., 1997). For future experiments, we will also consider alternative portable techniques, such as a dilution method (Davis et al., 1985; Kinar and Pomeroy, 2015; Mitterer, 2016).

## 4 Conclusions

We focused on the systematic observation of capillary barriers and associated preferential flow during laboratory experiments in a cold chamber. We sieved nine samples of finer-over-coarser snow. These samples were subjected to controlled supply of dyed water until water arrived at sample base. Liquid water patterns in stratified snow were characterized using visual inspection, LWC measurements and horizontal sectioning. Results were also compared with SNOWPACK simulations.

Overall, results confirmed that a finer-over-coarser transition in snow layering causes ponding of water when this comes at the textural boundary. Measured peaks in LWC over the boundary are large with respect to usual measurements in the field (up to  $\sim 33$  vol% in FC samples and  $\sim 34 - 36$  vol% in FM samples), while peaks in MC samples are usually  $\leq 10$  vol%. Differences in peak LWC between samples were explained basing on retention properties of snow with different grain size. A more detailed analysis of horizontal sections revealed marked variability of wetness conditions at cm scale, thus suggesting that local LWC might even reach saturated conditions, as expected by a simple estimation of LWC at water entry suction.

Horizontal sectioning of samples confirmed that preferential flow seems the dominant process in water transmission in snow. The area occupied by fingers ( $f$ ) increases with grain size, while no definitive result was obtained to establish a relation between  $f$  and water input rate. This is explained by the strong perturbation introduced by the capillary barrier in liquid water patterns if compared with previous observations in homogeneous snow.

The comparison with SNOWPACK showed that, in general terms, the implementation of Richards equation clearly reproduces the existence of a capillary barrier and yields a good agreement with observed peaks in LWC at the interface. A discussion of observed and simulated LWC revealed possible discrepancies between point conditions and 3D patterns even at cm scale.

## 5 Author contribution

Francesco Avanzi, Hiroyuki Hirashima and Satoru Yamaguchi designed the experiments, Francesco Avanzi and Satoru Yamaguchi performed the experiments, Hiroyuki Hirashima performed SNOWPACK simulations, Francesco Avanzi prepared the manuscript with the contribution of all coauthors.

*Acknowledgements.* Fruitful discussions about this work with Dr. Atsushi Sato and Dr. Yoshiyuki Ishii are acknowledged. We would like to thank the staff of the Snow and Ice Research Center, National Research Institute for Earth Science and Disaster Prevention, for helpful discussions. FA is grateful for the support received during his research period at the Snow and Ice Research Center in Nagaoka. We would like to thank Mr. Sugai Yusuke for his assistance during experimental activities. We acknowledge the Editor Dr. Guillaume Chambon, Dr. Christoph Mitterer, and an anonymous referee for their constructive comments on the manuscript.

## References

- Abramoff, M. D., Magalhães, P. J., and Ram, S. J.: Image Processing using ImageJ, *Biophotonics international*, 11, 36–43, 2004.
- Adachi, S., Yamaguchi, S., Ozeki, T., and Kose, K.: Hysteresis in the water retention curve of snow measured  
485 using an MRI system, in: Proceedings to the 2012 International Snow Science Workshop, Anchorage, Alaska, 2012.
- Avanzi, F., Caruso, M., Jommi, C., De Michele, C., and Ghezzi, A.: Continuous-time monitoring of liquid water content in snowpacks using capacitance probes: A preliminary feasibility study, *Advances in Water Resources*, 68, 32–41, doi:10.1016/j.advwatres.2014.02.012, 2014.
- 490 Avanzi, F., Yamaguchi, S., Hirashima, H., and De Michele, C.: Bulk volumetric liquid water content in a seasonal snowpack: modeling its dynamics in different climatic conditions, *Advances in Water Resources*, 2015.
- Baggi, S. and Schweizer, J.: Characteristics of wet-snow avalanche activity: 20 years of observations from a high alpine valley (Dischma, Switzerland), *Natural Hazards*, 50, 97–108, 2008.
- Baker, R. S. and Hillel, D.: Laboratory tests of a theory of fingering during infiltration into layered soils, *Soil*  
495 *Sci. Soc. Am. J.*, 54, 20–30, 1990.
- Bartelt, P. and Lehning, M.: A physical SNOWPACK model for the Swiss avalanche warning Part I: numerical model, *Cold Regions Science and Technology*, 35, 123–145, doi:10.1016/S0165-232X(02)00074-5, 2002.
- Baver, C. E., Parlange, J. Y., Stoof, C. R., DiCarlo, D. A., Wallach, R., Durnford, D. S., and Steenhuis, T. S.: Capillary pressure overshoot for unstable wetting fronts is explained by Hoffman’s velocity-dependent  
500 contact-angle relationship, *Water Resources Research*, 50, 5290–5297, 2014.
- Blöschl, G.: Scaling issues in snow hydrology, *Hydrological Processes*, 1999.
- Brun, E.: Investigation on wet-snow metamorphism in respect of liquid-water content, *Annals of Glaciology*, 13, 22–26, 1989.
- Colbeck, S. C.: A theory of water percolation in snow, *Journal of Glaciology*, 11, 369–385, 1972.
- 505 Colbeck, S. C.: The difficulties of measuring the water saturation and porosity of snow, *Journal of Glaciology*, 20, 189 – 201, 1978.
- Daanen, R. P. and Nieber, J. L.: Model for Coupled Liquid Water Flow and Heat Transport with Phase Change in a Snowpack, *J. Cold Reg. Engrg.*, 23, 43–68, 2009.
- Davis, R. E., Dozier, J., LaChapelle, E. R., and Perla, R.: Field and Laboratory Measurements of Snow Liquid  
510 Water by Dilution, *Water Resources Research*, 21, 1415–1420, 1985.
- de Rooij, G. H.: Modeling fingered flow of water in soils owing to wetting front instability: a review, *Journal of Hydrology*, 231-232, 277–294, 2000.
- DeWalle, D. R. and Rango, A.: Principles of Snow Hydrology, Cambridge University Press, 2011.
- DiCarlo, D. A.: Experimental measurements of saturation overshoot on infiltration, *Water Resources Research*,  
515 40, W04 215, 2004.
- DiCarlo, D. A.: Capillary pressure overshoot as a function of imbibition flux and initial water content, *Water Resources Research*, 43, W08 402, 2007.
- DiCarlo, D. A.: Stability of gravity-driven multiphase flow in porous media: 40 years of advancements, *Water Resources Research*, 49, 4531–4544, 2013.

- 520 Dietz, A. J., Kuenzer, C., Gessner, U., and Dech, S.: Remote sensing of snow - a review of available methods, *International Journal of Remote Sensing*, 33, 4094 – 4134, doi:10.1080/01431161.2011.640964, 2012.
- Egorov, A. G., Dautov, R. Z., Nieber, J. L., and Sheshukov, A. Y.: Stability analysis of gravity-driven infiltrating flow, *Water Resources Research*, 39, 1266, 2003.
- Eiriksson, D., Whitson, M., Luce, C. H., Marshall, H. P., Bradford, J., Benner, S. G., Black, T., Hetrick, H., and  
525 McNamara, P.: An evaluation of the hydrologic relevance of lateral flow in snow at hillslope and catchment scales, *Hydrological Processes*, 27, 640–654, doi:10.1002/hyp.9666, 2013.
- Fierz, C. and Föhn, P. M. B.: Long - term observation of the water content of an alpine snowpack, in: *Proceedings of the International Snow Science Workshop*, 30 October - 3 November 1994, Snowbird, Utah, 1995.
- 530 Fierz, C., Armstrong, R., Durand, Y., Etchevers, P., Greene, E., McClung, D., Nishimura, K., Satyawali, P., and Sokratov, S.: *The International Classification for Seasonal Snow on the Ground*, Tech. rep., IHP-VII Technical Documents in Hydrology N 83, IACS Contribution N 1, UNESCO - IHP, Paris, 2009.
- Forster, R. R., Box, J. E., van den Broeke, M. R., Miegge, C., Burgess, E. W., van Angelen, J. H., Lenaerts, J. T. M., Koenig, L. S., Paden, J., Lewis, C., Prasad Gogineni, S., Leuschen, C., and McConnell, J. R.: Extensive  
535 liquid meltwater storage in firn within the Greenland ice sheet, *Nature Geoscience*, 7, 95–98, 2014.
- Harper, J., Humphrey, N., Pfeffer, W. T., Brown, J., and Fettweis, X.: Greenland ice - sheet contribution to sea - level rise buffered by meltwater storage in firn, *Nature*, 491, 240 – 243, 2012.
- Heilig, A., Eisen, O., and Schneebeli, M.: Temporal observations of a seasonal snowpack using upward-looking GPR, *Hydrological Processes*, 24, 3133–3145, 2010.
- 540 Heilig, A., Mitterer, C., Schmid, L., Wever, N., Schweizer, J., Marshall, H.-P., and Eisen, O.: Seasonal and diurnal cycles of liquid water in snow - measurements and modeling, *Journal of Geophysical Research - Earth Surface*, 2015.
- Hill, D. E. and Parlange, J.-Y.: Wetting front instability in layered soils, *Soil Science Society of America Proceedings*, 36, 697–02, 1972.
- 545 Hillel, D. and Baker, R. S.: A descriptive theory of fingering during infiltration into layered soils, *Soil Science*, 146, 51–55, 1988.
- Hirashima, H., Yamaguchi, S., Sato, A., and Lehning, M.: Numerical modeling of liquid water movement through layered snow based on new measurements of the water retention curve, *Cold Regions Science and Technology*, 64, 94–103, doi:10.1016/j.coldregions.2010.09.003, 2010.
- 550 Hirashima, H., Yamaguchi, S., and Katsushima, T.: A multi-dimensional water transport model to reproduce preferential flow in the snowpack, *Cold Regions Science and Technology*, 108, 80–90, 2014.
- Jordan, R.: Effects of capillary discontinuities on water flow and water retention in layered snowcovers, *Defence Science Journal*, 45, 79–91, 1995.
- Katsushima, T., Kumakura, T., and Takeuchi, Y.: A multiple snow layer model including a parameteriza-  
555 tion of vertical water channel process in snowpack, *Cold Regions Science and Technology*, 59, 143–151, doi:10.1016/j.coldregions.2009.09.002, 2009a.
- Katsushima, T., Yamaguchi, S., Kumakura, T., and Sato, A.: Measurement of dynamic water entry value for dry snow, in: *Proceedings to the International Snow Science Workshop 2009*, Davos, Switzerland, 2009b.



Katsushima, T., Yamaguchi, S., Kumakura, T., and Sato, A.: Experimental analysis of preferential flow in  
560 dry snowpack, *Cold Regions Science and Technology*, 85, 206–216, doi:10.1016/j.coldregions.2012.09.012,  
2013.

Kawashima, K., Endo, T., and Takeuchi, Y.: A portable calorimeter for measuring liquid-water content of wet  
snow, *Annals of Glaciology*, 26, 103–106, 1998.

Kinar, N. J. and Pomeroy, J. W.: SAS2: the system for acoustic sensing of snow, *Hydrological Processes*, 29,  
565 4032–4050, 2015.

Lehning, M., Völksch, I., Gustafsson, D., Nguyen, T. A., Stähli, M., and Zappa, M.: ALPINE3D: a detailed  
model of mountain surface processes and its application to snow hydrology, *Hydrological Processes*, 20,  
2111–2128, doi:10.1002/hyp.6204, 2006.

Liu, Y., Steenhuis, T. S., and Parlange, J.-Y.: Formation and persistence of fingered flow fields in coarse grained  
570 soils under different moisture contents, *Journal of Hydrology*, 159, 187 – 195, 1994.

Lundquist, J. D. and Dettinger, M. D.: How snowpack heterogeneity affects diurnal streamflow timing, *Water  
Resources Research*, 41, W05 007, doi:10.1029/2004WR003649, 2005.

Machguth, H., MacFerrin, M., van As, D., Box, J. E., Charalampidis, C., Colgan, W., Fausto, R. S., Meijer,  
H. A. J., Mosley-Thompson, E., and van de Wal, R. S. W.: Greenland meltwater storage in firn limited by  
575 near-surface ice formation, *Nature Climate Change*, doi:10.1038/nclimate2899, 2016.

Marsh, P. and Woo, M.: Meltwater movement in natural heterogeneous snow covers, *Water Resources Research*,  
21, 1710–1716, doi:10.1029/WR021i011p01710, 1985.

Marsh, P. and Woo, M.-K.: Wetting front advance and freezing of meltwater within a snow cover 1. Observations  
in the Canadian Arctic, *Water Resources Research*, 20, 1853–1864, doi:10.1029/WR020i012p01853, 1984a.

580 Marsh, P. and Woo, M.-K.: Wetting front advance and freezing of meltwater within a snow cover 2. A simulation  
model, *Water Resources Research*, 20, 1865–1874, doi:10.1029/WR020i012p01865, 1984b.

Marshall, H. P., Conway, H., and Rasmussen, L. A.: Snow densification during rain, *Cold Regions Science and  
Technology*, 30, 35–41, 1999.

McGurk, B. J. and Marsh, P.: Flow-finger continuity in serial thick-sections in a melting Sierran snowpack, in:  
585 *Biogeochemistry of Seasonally Snow-Covered Catchments (Proceedings of a Boulder Symposium)*, 1995.

Mitterer, C.: Interactive comment on Laboratory-based observations of capillary barriers and preferential flow  
in layered snow by F. Avanzi et al., *The Cryosphere Discuss.*, 9, C2938–C2949, 2016.

Mitterer, C. and Schweizer, J.: Analysis of the snow-atmosphere energy balance during wet-  
snow instabilities and implications for avalanche prediction, *The Cryosphere*, 7, 205 – 216,  
590 <http://www.the-cryosphere.net/7/205/2013/>, 2013.

Mitterer, C., Hirashima, H., and Schweizer, J.: Wet-snow instabilities: comparison of measured and modelled  
liquid water content and snow stratigraphy, *Annals of Glaciology*, 52, 201 – 208, 2011.

Mitterer, C., Techel, F., Fierz, C., and Schweizer, J.: An operational supporting tool for assessing wet-snow  
avalanche danger, in: *International Snow Science Workshop Grenoble - Chamonix Mont-Blanc - 2013*, 2013.

595 Peitzsch, E., Birkeland, K. W., and Hansen, K. J.: Water movement and capillary barriers in a stratified and  
inclined snowpack, in: *Proceedings of the 2008 International Snow Science Workshop*, Whistler, British  
Columbia, 2008.

- Pfeffer, W. T. and Humphrey, N. F.: Determination of timing and location of water movement and ice-layer formation by temperature measurements in sub-freezing snow, *Journal of Glaciology*, 42, 292–304, 1996.
- 600 Pfeffer, W. T., Illangasekare, T. H., and Meier, M. F.: Analysis and modeling of melt-water refreezing in dry snow, *Journal of Glaciology*, 36, 238–246, 1990.
- Saffman, P. and Taylor, G.: The penetration of a fluid into a porous medium or Hele-Shaw cell containing a more viscous fluid, *Proc. R. Soc. London*, 245, 312–329, 1958.
- Schmid, L., Koch, F., Heilig, A., Prasch, M., Eisen, O., Mauser, W., and Schweizer, J.: A novel sensor combination (upGPR - GPS) to continuously and nondestructively derive snow cover properties, *Geophysical Research Letters*, 42, 1 – 9, 2015.
- 605 Schmid, L., Koch, F., Heilig, A., Prasch, M., Eisen, O., Mauser, W., and Schweizer, J.: A novel sensor combination (upGPR - GPS) to continuously and nondestructively derive snow cover properties, *Geophysical Research Letters*, 42, 1 – 9, 2015.
- Schneebeili, M.: Development and stability of preferential flow paths in a layered snowpack, in: *Biogeochemistry of Seasonally Snow-Covered Catchments (Proceedings of a Boulder Symposium)*, IAHS Publ. no. 228, 1995.
- 610 Stein, J., Laberge, G., and Lévesque, D.: "Monitoring the dry density and the liquid water content of snow using time domain reflectometry (TDR)", *Cold Regions Science and Technology*, 25, 123 – 136, 1997.
- Techel, F. and Pielmeier, C.: Point observations of liquid water content in wet snow - investigating methodical, spatial and temporal aspects, *The Cryosphere*, 5, 405–418, doi:10.5194/tc-5-405-2011, <http://www.the-cryosphere.net/5/405/2011/>, 2011.
- 615 Techel, F., Pielmeier, C., and Schneebeili, M.: Microstructural resistance of snow following first wetting, *Cold Regions Science and Technology*, 65, 382–391, doi:10.1016/j.coldregions.2010.12.006, 2011.
- van Genuchten, M. T.: A Closed-form Equation for Predicting the Hydraulic Conductivity of Unsaturated Soils, *Soil Sci. Soc. Am. J.*, 44, 892–898, 1980.
- Wakahama, G.: The infiltration of melt water into snow cover 1 (in Japanese, with English Abstr.), *Tech. rep., Low Temperature Science, Series A 21*, 45-74, 1963.
- 620 Waldner, P. A., Schneebeili, M., Schultze-Zimmermann, U., and Flühler, H.: Effect of snow structure on water flow and solute transport, *Hydrological Processes*, 18, 1271–1290, doi:10.1002/hyp.1401, 2004.
- Walter, B., Horender, S., Gromke, C., and Lehning, M.: Measurements of the pore-scale water flow through snow using Fluorescent Particle Tracking Velocimetry, *Water Resources Research*, 49, 2013.
- 625 Wankiewicz, A.: A review of water movement in snow, in: *Modeling of snow cover runoff*, edited by Colbeck, S. C. and Ray, M., U.S. Army Cold Regions Research and Engineering Laboratory, Hanover, New Hampshire, 1978.
- Weitz, D. A., Stokes, J. P., Ball, R. C., and Kushnick, A. P.: Dynamic Capillary Pressure in Porous Media: Origin of the Viscous-Fingering Length Scale, *Phys. Rev. Lett.*, 59, 2967, 1987.
- 630 Wever, N., Fierz, C., Mitterer, C., Hirashima, H., and Lehning, M.: Solving Richards Equation for snow improves snowpack meltwater runoff estimations in detailed multi-layer snowpack model, *The Cryosphere*, 8, 257–274, doi:10.5194/tc-8-257-2014, <http://www.the-cryosphere.net/8/257/2014/>, 2014.
- Wever, N., Schmid, L., Heilig, A., Eisen, O., Fierz, C., and Lehning, M.: Verification of the multi-layer SNOWPACK model with different water transport schemes, *The Cryosphere Discussions*, 9, 2655–2707, doi:10.5194/tcd-9-2655-2015, 2015.
- 635 Wever, N., Vera Valero, C., and Fierz, C.: Assessing wet snow avalanche activity using detailed physics based snowpack simulations, *Geophysical Research Letters*, 2016.

- Williams, M. W., Erickson, T. A., and Petzelka, J. L.: Visualizing meltwater flow through snow at the centimetre-to-metre scale using a snow guillotine, *Hydrological Processes*, 24, 2098 – 2110, 2010.
- 640 Yamaguchi, S., Katsushima, T., Sato, A., and Kumakura, T.: Water retention curve of snow with different grain sizes, *Cold Regions Science and Technology*, 64, 87–93, doi:10.1016/j.coldregions.2010.05.008, 2010.
- Yamaguchi, S., Watanabe, K., Katsushima, T., Sato, A., and Kumakura, T.: Dependence of the water retention curve of snow on snow characteristics, *Annals of Glaciology*, 53, 6–12, doi:http://dx.doi.org/10.3189/2012AoG61A001, 2012.
- 645 Yosida, Z.: A calorimeter for measuring the free water content of wet snow, *Journal of Glaciology*, 3, 574–576, 1960.

**Table 1.** Experimental details.  $W$  is the applied water input rate,  $\rho_{D,U}$  is the dry density of the upper layer,  $\rho_{D,L}$  is the dry density of the lower layer.

<b>Sample ID</b>	$W$ (mm/h)	$W$ (g/min)	$\rho_{D,U}$ (kg/m <sup>3</sup> )	$\rho_{D,L}$ (kg/m <sup>3</sup> )	<b>Upper layer</b> thickness (cm)	<b>Lower layer</b> thickness (cm)
FC1	11.9	0.39	417	465	10	10
FC2	28	0.92	449	483	10	8
FC3	113	3.7	433	470	10	10
FM1	11.9	0.39	444	484	10	10
FM2	27.7	0.91	442	487	10	8
FM3	110	3.6	455	510	10	10
MC1	11	0.36	472	487	10	10
MC2	27.3	0.89	498	480	10	8
MC3	111	3.6	494	478	10	10

**Table 2.** Experimental results: observed ponding layer thickness  $p$ , experiment duration  $t_t$ , specific travel time  $\tau$ . As for  $p$ , approximated lower and upper values are reported due to spatial heterogeneity in this variable.

<b>Sample ID</b>	<b><math>p</math> (min - max)</b>	<b><math>t_t</math></b>	<b><math>\tau</math></b>
	<b>(cm)</b>	<b>(min)</b>	<b>(min/cm)</b>
FC1	2 - 3	92	4.6
FC2	3 - 4	50	2.8
FC3	2 - 3	14.5	0.725
FM1	2 - 3	90	4.5
FM2	2 - 3	40	2.2
FM3	1 - 2	13.5	0.675
MC1	0 - 1	8	0.4
MC2	1 - 1	8.45	0.47
MC3	0.5 - 1	5.3	0.265

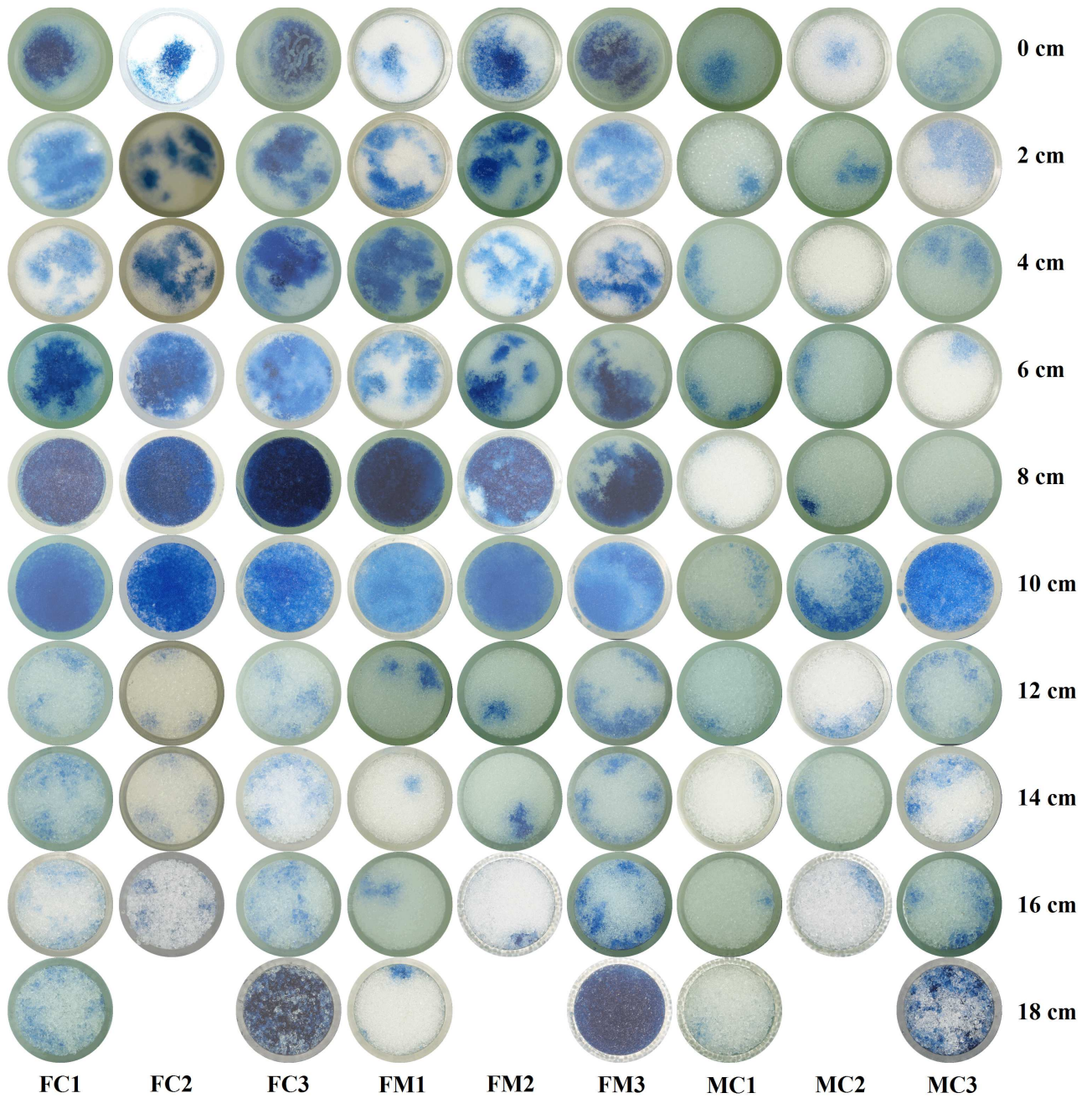


**Figure 1.** Sections of all the samples (rings diameter equal to 5 cm, 2 cm vertical resolution) at the end of each experiment. Each column refers to a different sample (as indicated in the last row), while each row refers to the same depth from sample top surface (depth indicated by the number on the right side of each row). For all the samples, the texture boundary between different grain sizes is located at a depth equal to 10 cm.

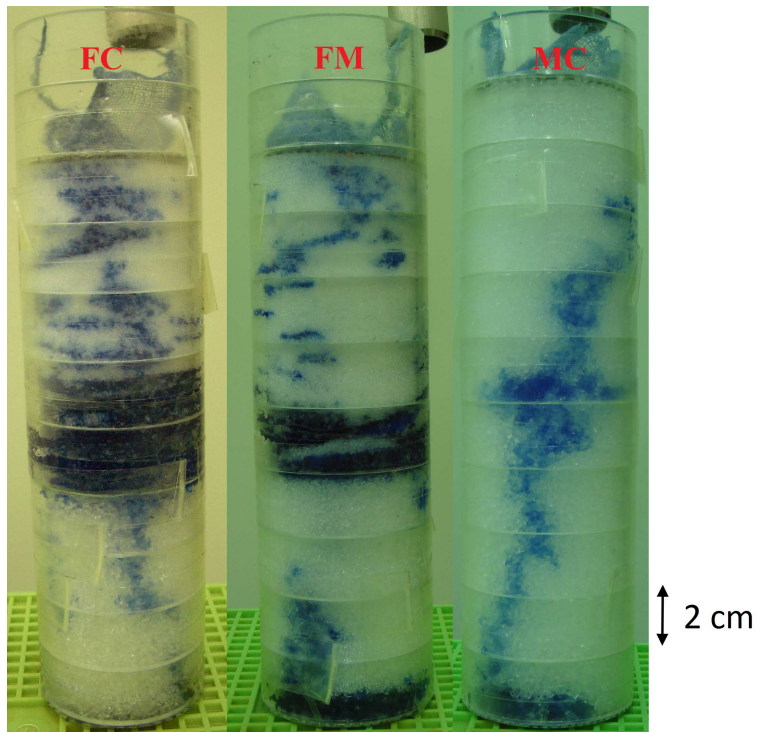


**Figure 2.** Three samples at the end of the experiments: FC2 (on the left, as an example of FC samples), FM2 (at the center, as an example of FM samples) and MC1 (on the right, as an example of MC samples).

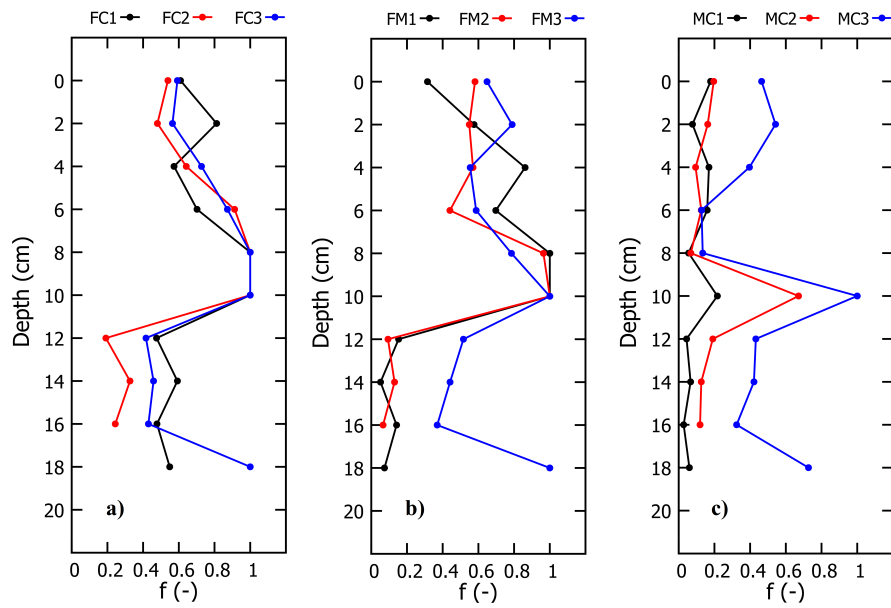


**Figure 3.** Measured  $f$  profiles.  $f$  is the ratio between wet and total area for all the sections in Fig. 1. Panel (a): FC samples; panel (b): FM samples; panel (c): MC samples. The vertical coordinate refers to the depth of the section from sample top surface.



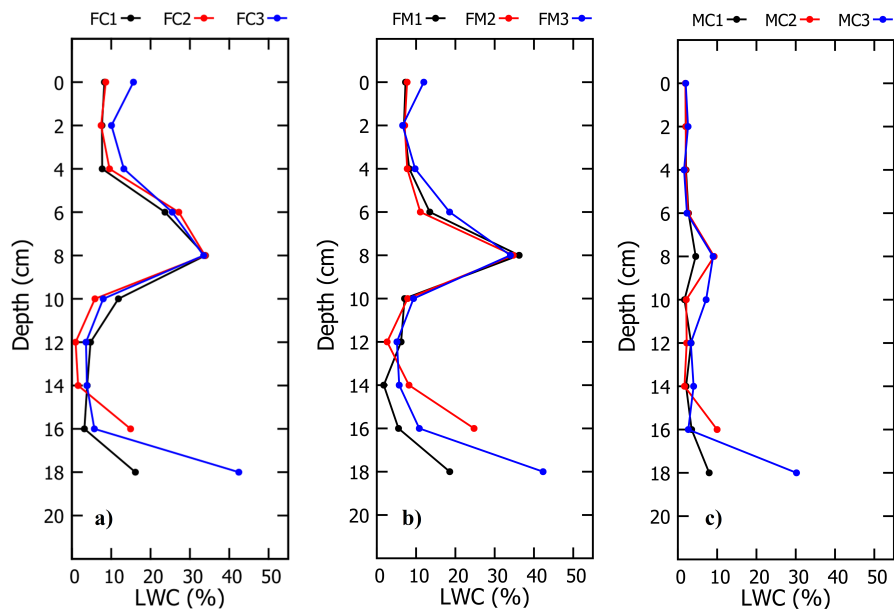


**Figure 4.** Measured LWC (vol %). Panel (a): FC samples; panel (b): FM samples; panel (c): MC samples. Each point represents bulk LWC in the underlying 2 cm. This convention is consistent with Fig. 1 and 3.

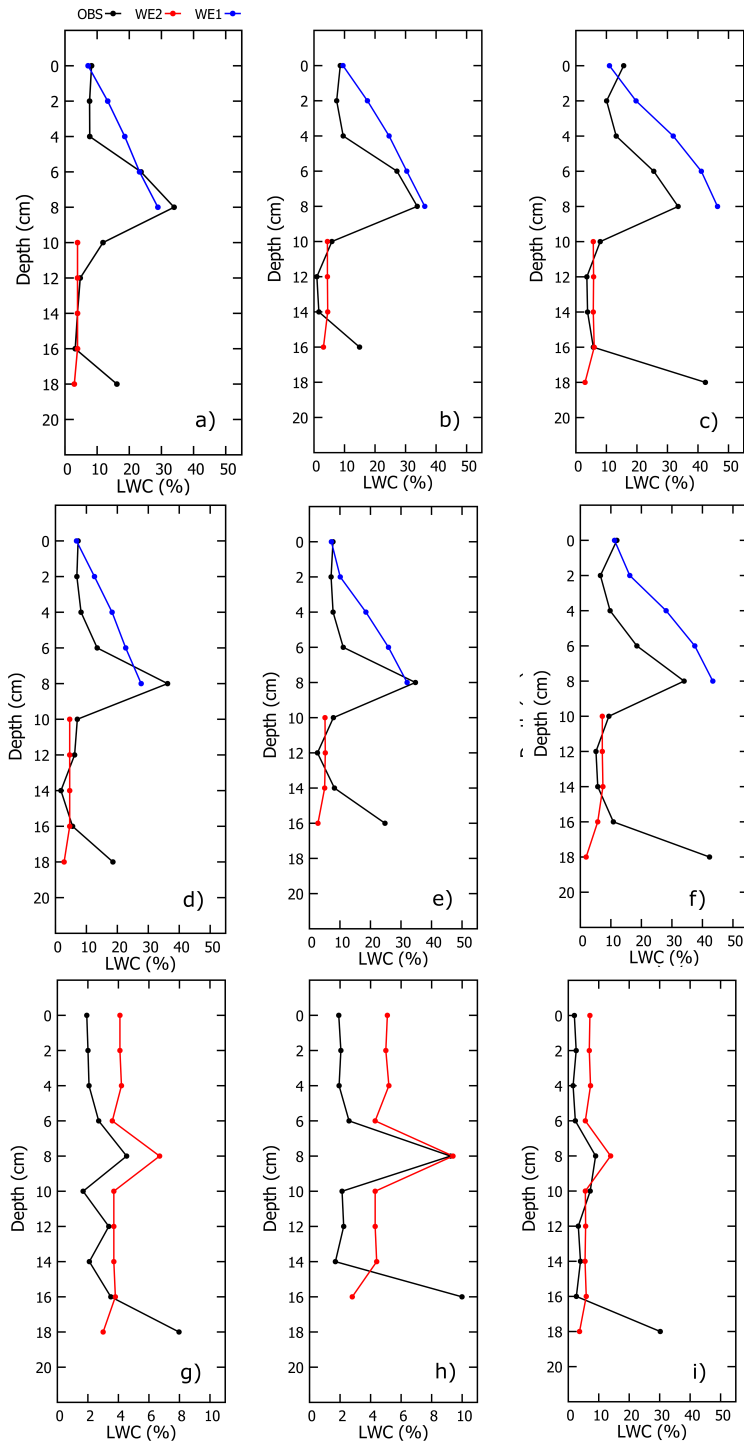


**Figure 5.** Comparison between observed and simulated profiles of volumetric LWC. Panels (a), (b) and (c) refer to samples FC1, FC2 and FC3. Panels (d), (e) and (f) refer to samples FM1, FM2 and FM3. Panels (g), (h) and (i) refer to samples MC1, MC2 and MC3. Note that panels (g) and (h) have a different horizontal range from the others. Each point represents bulk LWC in the underlying 2 cm.